ACS APPLIED MATERIALS & INTERFACES

www.acsami.org

Research Article

Nanoporous PVDF Hollow Fiber Employed Piezo−Tribo Nanogenerator for Effective Acoustic Harvesting

Zhaohan Yu, Ming Chen, Yunming Wang,* Jiaqi Zheng, Yongkang Zhang, Huamin Zhou, and Dequn Li

Cite This: *ACS Appl. Mater. Interfaces* 2021, 13, 26981−26988

Read Online

ACCESS | Metrics & More | Article Recommendations | Supporting Information

ABSTRACT: Restricted by the inherent property of low power density, acoustic energy can hardly be effectively captured by conventional piezo- or triboelectric nanogenerators for powering miniature electronics. Herein, a novel piezo−tribo hybrid nanogenerator employing nanoporous polyvinylidene fluoride (PVDF) hollow fiber and polydimethylsiloxane (PDMS) valve, which can mimic the eardrum, has been advocated for efficient acoustic harvesting. The nanoporous, hollow, and valve structure design, together with the effective combination of piezo- and triboelectricity, make the nanoporous PVDF hollow fiber and PDMS valve based acoustic harvester (PHVAH) a promising candidate for acoustic−electric conversion. With an optimal output of 105.5 V and 16.7 μA and a power density of 0.92 W m^{-2} under the sound stimulation of 117.6 dB and 150 Hz, it can not only recognize audio signals but also convert the sound into electrical energy to light up seven LED bulbs in series. Exhibiting excellent durability and stability, the disruptive innovation proposed here is an effective method for hunting the ubiquitous sound energy in the environment, which provides great potential and impetus for using acoustic−electric conversion to power various low-power-consumption sensors.

KEYWORDS: *PVDF nanoporous hollow fiber, PDMS valve, acoustic harvest, piezo−triboelectric, coaxial electrospinning*

1. INTRODUCTION

The emerging development of the Internet of Things puts forward stringent requirements for the power supply of truly autonomous MEMS electronics based on lightweight, portable, and sustainable needs.[1−4] As a potential solution, the effective conversion of ubiquitous mechanical energy in the environment to available electricity for powering such devices has attracted growing attention.[5,6] Acoustic energy, with the unique and attractive features of being widely distributed, sustainable, and clean, is an excellent resource for such applications, especially in biomonitoring, biometric system, and entrance and mobile control.[7,8] However, limited by the inherent low power density characteristics and broad bandwidth, sound can hardly be captured by traditional piezo- or triboelectric energy conversion equipment.[9,10] To realize the utilization of sound energy, a number of attempts have been made to improve the sensitivity of nanogenerators.[11−16] The widely accepted approach is to increase the porosity of the material, which can be achieved by electrospinning and material etching, thereby reducing the modulus and increasing the deformation and, in turn, improving the energy conversion efficiency.[17−20] But, it is still insufficient for the effective collection of weak sound signals. For this reason, the design of external structures such as cantilever beams or resonant cavities is exploited to amplify the deformation of the energy conversion device.[21−23] Though the structural design does provide improved sensitivity in energy harvest, it also brings problems to the flexibility and stability of the device. Therefore, the realization of the efficient and continuous collection of sound energy requires a strategy to fabricate sound−electric conversion equipment with excellent performance as well as a stable and flexible structure, which still poses an urgent problem in acoustic acquisition.[24]

To meet these challenges and effectively convert such a promising energy into electricity, we propose a novel type of acoustic harvester (AH) with the structure of nanoporous polyvinylidene fluoride (PVDF) hollow fiber and polydimethylsiloxane (PDMS) valve (PHV) fabricated by coaxial electrospinning. The nanoporous PVDF hollow fiber (PH) membrane prepared by coaxial electrospinning can serve as a high-efficiency piezo nanogenerator with high porosity and β content, as well as a scaffold for the PDMS valve. The thin valve will generate giant vibrations even under the weak irritation of acoustic waves, thereby producing an extra triboelectric output. The effective combination of piezo- and

Received: March 9, 2021
Accepted: May 24, 2021
Published: June 7, 2021

https://doi.org/10.1021/acsami.1c04489
ACS Appl. Mater. Interfaces 2021, 13, 26981−26988

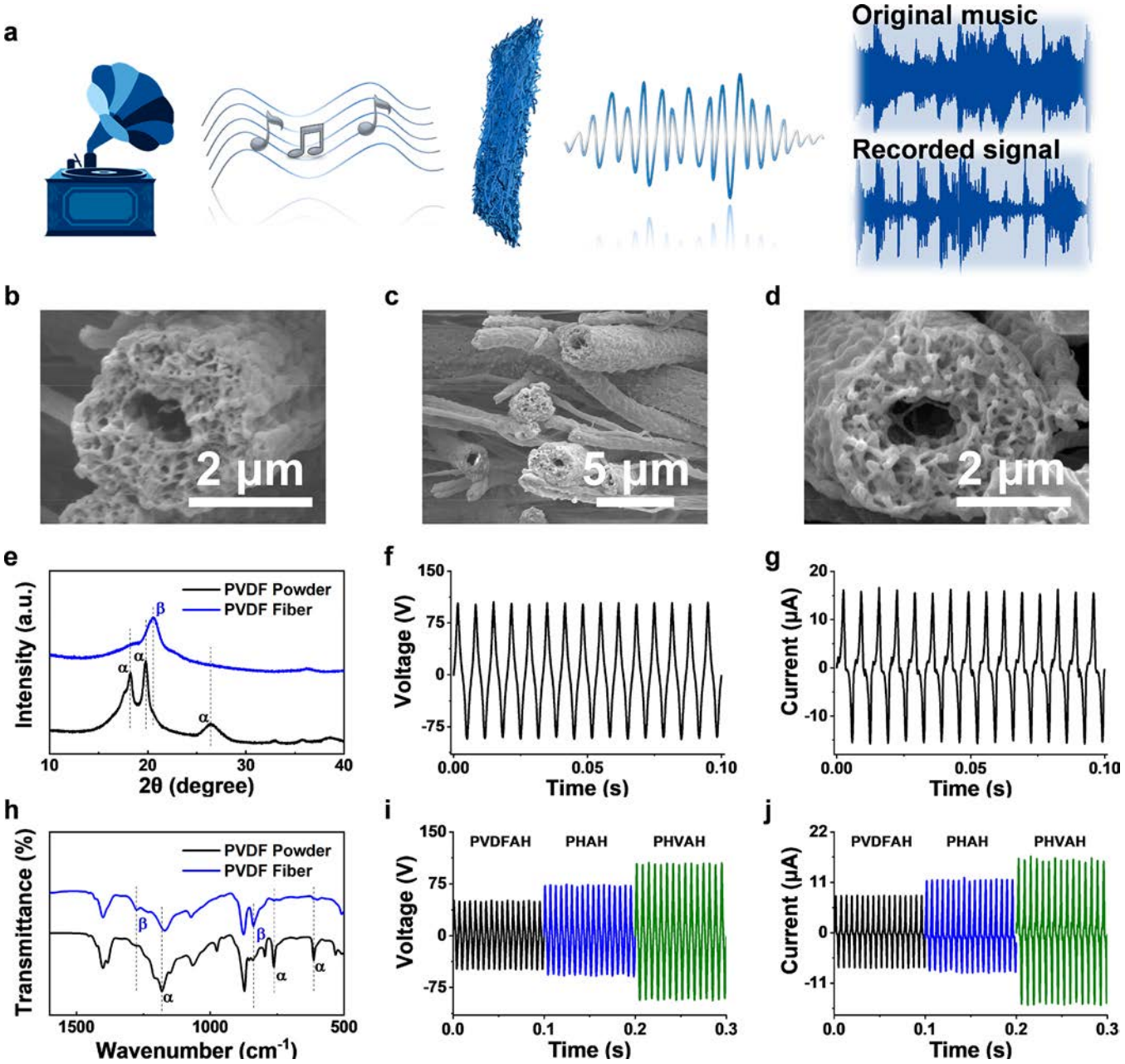

Figure 1. (a) Schematic diagram of the realization from sound to electricity with the fabricated PHVAH. (b) Morphology of single PH fiber. (c) Morphology of PH fibers. (d) Morphology of PVDF fiber with PDMS valves. (e) X-ray diffraction (XRD) pictures of PVDF powder and PVDF fiber prepared by coaxial electrospinning. (f) Optimal output voltage of PHVAH under a sound stimulus of 117.6 dB and 150 Hz. (g) Optimal output current of PHVAH under a sound stimulus of 117.6 dB and 150 Hz. (h) Fourier-transform infrared spectra (FTIR) images of PVDF powder and PVDF fiber. (i) Output voltages of PVDFAH, PHAH, and PHVAH under a sound stimulus of 117.6 dB and 150 Hz. (j) Output currents of PVDFAH, PHAH, and PHVAH under a sound stimulus of 117.6 dB and 150 Hz.

triboelectricity makes the nanoporous PVDF hollow fiber and PDMS valve based acoustic harvester (PHVAH) a good conductor of sound and a promising candidate for acoustic energy collection.[25] The optimal performance of PHVAH reaches 105.5 V and 16.7 μA at a sound stimulation of 150 Hz and 117.6 dB, while the power density is 0.92 W m^{-2}. In additon to identifing and restoring audio signals, it can also harvest energy to light up seven LED bulbs connected in a series in a 'V' shape. With a collection of effective, wearable, lightweight, and easy to fabricate, the disruptive design of PVHAH not only unveils a new strategy for the fabrication of high-efficiency energy conversion devices but also takes a significant step forward toward their potential application in acoustic harvesting and self-powered artificial auditory sensors.

2. RESULTS AND DISCUSSION

The PHVAH proposed here allows for effective conversion from sound to electricity, and the detailed schematic diagram is shown in Figure 1a. The PVDF membrane with a nanoporous and hollow fiber structure (Figure 1b,c) was obtained after removing the polyethylene glycol (PEG) in the PVDF/PEG coaxial fiber prepared by coaxial electrospinning (Figure S1). Then, by being immersed in the diluted PDMS, the PDMS valve structure was formed between the hollow fibers (Figure

https://doi.org/10.1021/acsami.1c04489
ACS Appl. Mater. Interfaces 2021, 13, 26981−26988

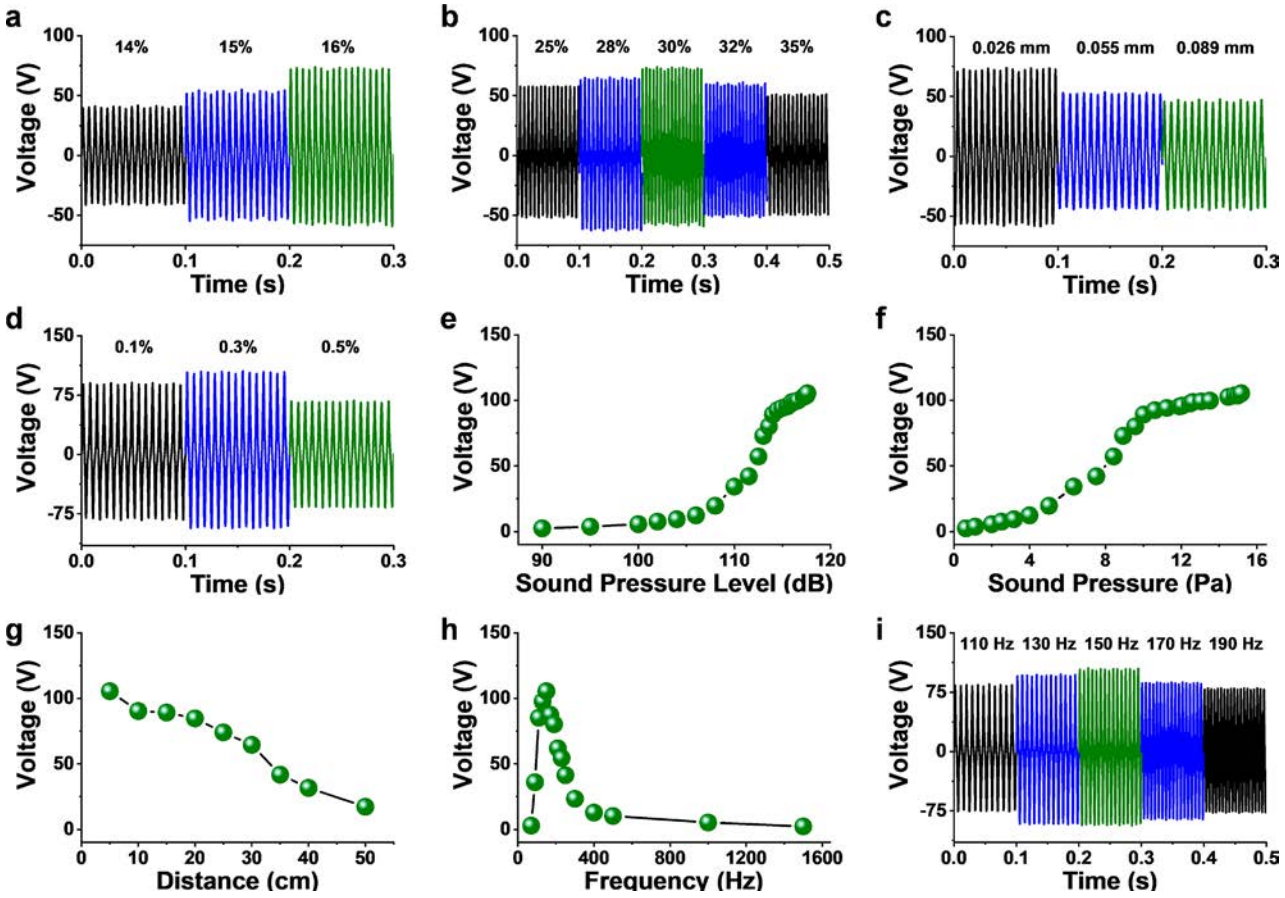

Figure 2. (a) Output voltage of devices fabricated with PH membrane at different concentrations of PVDF. (b) Output voltage of devices fabricated with PH membrane at different concentrations of PEG. (c) Responses of PHAH with different thicknesses of membrane. (d) Responses of PHVAH with different concentrations of PDMS. (e) Responses of PHVAH under different sound pressure levels at a frequency of 150 Hz. (f) Responses of PHVAH under different sound pressures at a frequency of 150 Hz. (g) Output performances of PHVAH at different distances from the sound source. (h) Responses of PHVAH under different frequencies at a sound pressure level of 117.6 dB. (i) Responses of PHVAH under frequencies from 110 to 190 Hz.

1d). With 30% w/v PEG and 16% w/v PVDF, a PH membrane with a hollow diameter of 1 μm can be fabricated, which exhibits a relatively excellent performance in acoustic harvesting. Additionally, due to the delayer demixing induced by the inner PEG solution, the hollow fibers exhibit a highly porous structure. Immersed in 0.3% PDMS, the ultrathin PDMS valves further improved the piezo−tribo properties as well as the sustainability of the device. All the above hollow, porous, and valve structures, together with the induced β-phase (Figure 1e,h) will certainly enhance the piezo−tribo performance. Parts f and g of Figure 2 demonstrate that the PHVAH is capable of delivering an optimal output performance of 105.5 V and 16.7 μA under a sound stimulus of 117.6 dB and 150 Hz, which is much higher than that of nanoporous PVDF hollow fiber based acoustic harvester (PHAH) (74.0 V, 12.0 μA) and pure PVDF fiber based acoustic harvester (PVDFAH) (51.1 V, 8.2 μA), as shown in Figure 1i,j. The distinct electrical output performance validates the feasibility of this structure in sound collection.

As a key factor associated with the properties of PHVAH, the morphology and size of the PVDF hollow fibers are of great importance. To ensure that the best hollow fiber is prepared for satisfactory performance, the regulation of the concentration of PVDF and PEG was investigated. For PVDF as the shell material, scanning electron microscopy (SEM) images in Figure S2 indicate that concentrations higher than 16% w/v or lower than 14% w/v can result in a failure of fiber morphology, including swelling and agglomeration. Within the range where the fiber can be uniformly formed, the output voltages are 41.9, 55.1, and 74.0 V corresponding to the concentrations of 14%, 15%, and 16% w/v, respectively (Figure 2a). As the functional component that generates the piezo−triboelectric response and serves as the scaffold of the membrane, too low a content of PVDF will be detrimental to output performance and cannot ensure the sustainability of the hollow fiber membrane. Therefore, considering both form and performance, 16% w/v is the optimal concentration for PVDF.

The doping and removal of PEG is also essential for the hollow and porous structure. The Fourier-transform infrared spectra (FTIR) characterization in Figure S3 indicates that the PEG doped in the PVDF fiber during coaxial spinning was successfully removed after washing; therefore, the hollow and porous structure was finally fabricated. In order to investigate the dominant mechanism of PEG in hollow fibers, the microstructure (Figure S4) and output properties (Figure 2b) of devices with different concentrations of PEG have been exhaustively studied. The higher the ratio, the larger the inner diameter and pore size of the hollow fiber, but too high a concentration will destroy the integrity of the fiber. The

https://doi.org/10.1021/acsami.1c04489
ACS Appl. Mater. Interfaces 2021, 13, 26981−26988

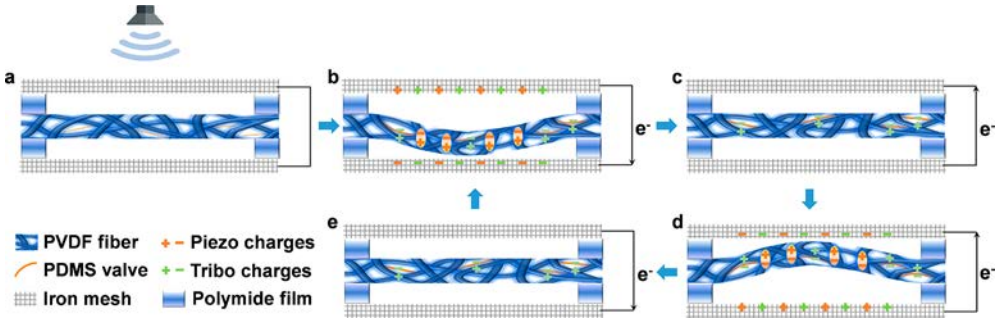

Figure 3. Structure illustration and mechanism diagram of PHVAH driven by sound: (a) Initial equilibrium state. (b) PHV membrane was deformed by sound waves. (c) Membrane recovers from the deformation. (d) PHV membrane was deformed by sound waves in the opposite direction. (e) Membrane recovers from the deformation again.

acoustic response performance of PVDF membranes with different hollow and porous fibers was further tested. The apparent investigation here demonstrates that the PVDF membrane prepared with 16% w/v PVDF and 30% w/v PEG solution has the optimal hollow and porous structure and thereby achieves the highest output performance.

To optimize the performance of the equipment, the design of the membrane macro structure is as important as the internal microstructure. The thickness is also an essential factor in determining the output performance of the PH membrane. To clarify the law, PH membranes with different thicknesses were fabricated and the corresponding output voltages were recorded. As shown in Figure 2c, the output voltage decreases from 74.0 to 47.7 V as the thickness increases from 0.026 to 0.089 mm. It can be interpreted that, for an acoustic harvester with a thicker membrane, a larger portion of the input will be absorbed by the membrane itself when the frequency and pressure of the sound stimulation are fixed. Analogous to a liner elastomer spring with a higher spring coefficient, a thicker film possessing a higher Young's modulus will generate less deformation and vibration in response to a specific stimulus, which consequently results in a lower output. Thus, a PH acoustic harvester with a thinner membrane as the functional layer can more effectively convert a voice into electricity.

Besides the hollow and porous design, the PDMS valves existing in the hollow fiber membrane also enhance the response to sound waves. To form an ultrathin valve structure that can produce strong vibrations when stimulated by the sound waves, the PDMS prepared with PDMS prepolymer and curing agent in a ratio of 10:1 needs to be further diluted with toluene. The results in Figure 2d and Figure S5 show that, compared with PHAH without PDMS (74.0 V, 12.0 μA), when the PDMS is scattered to 0.1%, 0.3%, and 0.5%, the corresponding output voltages of PHVAH are 90.9, 105.5, and 68.2 V and the currents are 13.1, 16.7, and 9.3 μA, respectively. This indicates that a proper addition of PDMS can indeed effectively increase the output of the AH. However, it should be noticed that the increase in PDMS concentration will lead to the clogging of pores and an increase in the thickness of the film (Figure S5c), which is not conducive to its deformation under weak acoustic stimulation, as discussed in the previous paragraph. At the appropriate concentration of 0.3%, ultrathin PDMS valves can be produced among the PVDF fibers. By imitating the human eardrum, the valves can generate continuous vibration under the stimulation of weak sound signals, thereby enhancing the vibration and deformation of the PHV membrane and, consequently, strengthening the piezo−triboelectric effect. Moreover, the PDMS valves rub against the PVDF hollow fiber, generating additional triboelectric output. In synergy with the above effects, PHVAH has been shown to exhibit superior sound collection capability with the structure of nanoporous PVDF hollow fibers and PDMS valves.

In addition to the design of the structure, the control of the crystal type also plays a crucial role in the performance of the device involving piezoelectric effects. It is widely acknowledged that the presence of the β-phase in PVDF is critical to the improvement of piezoelectric properties. Here, in the process of coaxial electrospinning, the high-voltage electric field applied to make the PVDF polymer droplets form a Taylor cone for the forming of membranes can simultaneously assist PVDF to complete the phase transition from α-phase to β-phase. As the XRD pattern in Figure 1e shows, untreated PVDF powder crystallized in nonpolar α-phase has obvious diffraction peaks at 18.24°, 19.80°, and 26.40°. But, it will be changed by the electric field in coaxial spinning, the α-phase diffraction peak disappeared in the PVDF membrane, and a new peak was formed at 20.59°, which was identified as β-phase.[26] To further characterize the phase transition, FTIR was also performed for analysis. Similar to the XRD results, the bands at 613, 762, and 975 cm^{-1} standing for α-phase in PVDF powder disappeared after spinning, and new bands representing β-phase appeared in the membrane at 838 and 1276 cm^{-1} instead (Figure 1h).[27] Completing an effective phase transformation from α to β in PVDF, coaxial electrospinning does contribute to the improvement of the acoustic−electric conversion capability of the device.

To further investigate the sensitivity of PHVAH to the response of sound, we simulated the practical application conditions of acoustic harvesting by changing the decibel, distance, and angle of sound separately and further evaluated the electrical performance. As shown in Figure 2e, when the sound increases from 90 to 117.6 dB, the corresponding output voltage of PHVAH rises from 2.4 to 105.5 V. The great increase in output comes from the greater deformation and vibration, which results from the rise in sound pressure from 0.63 to 15.17 Pa (Figure 2f and Equation S1). Likewise, when the sound source gradually approaches the device from a distance of 50 to 5 cm, the related converted piezo−triboelectric output increases from 17.3 to 105.5 V (Figure 2g). Besides, the SPL polar plots in Figure S6 indicate that angle is also influential and that the PHVAH is most sensitive to the sound from straight ahead. The remarkable changes in the response of PHVAH to different sounds demonstrate the

https://doi.org/10.1021/acsami.1c04489
ACS Appl. Mater. Interfaces 2021, 13, 26981−26988

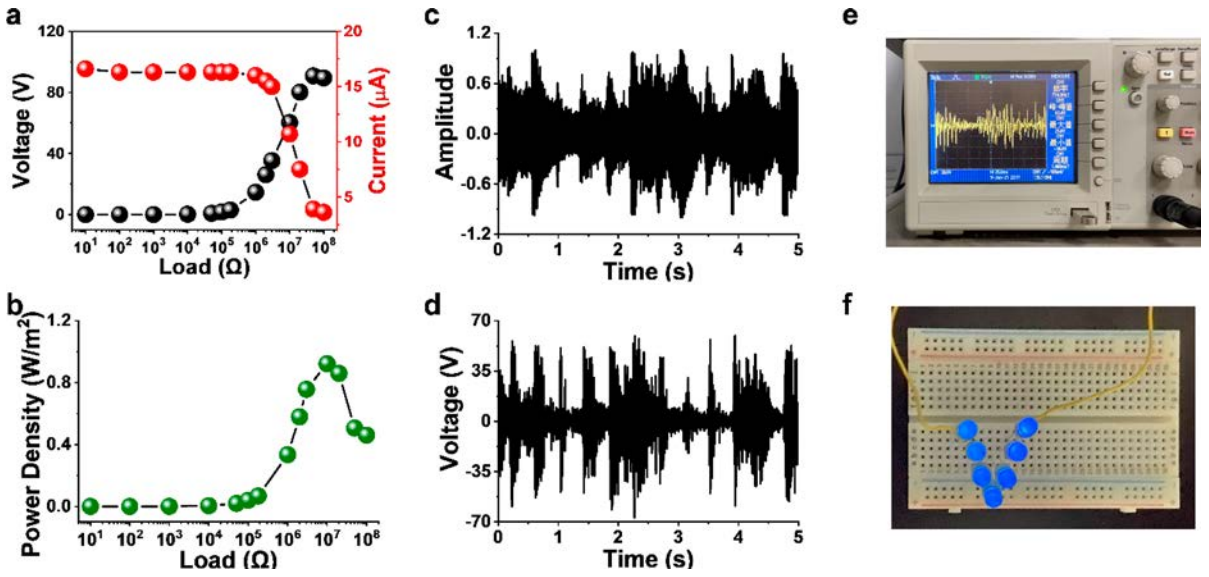

Figure 4. (a) Output voltages and currents of PHVAH with different external loading resistances. (b) Areal power densities of PHVAH with different external loading resistances. (c) Frequency spectrum of the music. (d) Changing output voltage of PHVAH when playing the music. (e) Photograph of the oscilloscope when playing the music. (f) LED bulbs in series are illuminated by PHVAH.

sensitivity of this device, which reveals its potential in sound harvest and even detection equipment.

It is widely acknowledged that, in addition to the insufficient sensitivity when detecting faint sounds, the most important factor that restricts the practical application of the existing nanogenerator in the field of sound wave collection is the selectivity of the equipment to the frequencies of sound. That is, they generally only perform well at a specific resonance frequency and the output decreases rapidly with the departure of frequency. To explore the potential of PHVAH working on a broad range of sound frequencies, its output performance was tested under different acoustic frequencies. As shown in Figure 2h, in a wide sound frequency range from 70 to 1500 Hz, the PHVAH has shown considerable sound acquisition performance. Particularly, at a frequency of 150 Hz, entering a resonant state, the PHVAH obtains a peak output of 105.5 V.[28] Moreover, in the range from 110 to 190 Hz, close to the resonance frequency of the PHV membrane to generate relatively great amplitudes, it corresponds to output voltages higher than 80 V (Figure 2i).[29] It has been proven that the PHVAH proposed here has a broad working frequency band, which provides considerable feasibility for its application of sound collection in more occasions.

The working mechanism of PHVAH is schematically depicted in Figure 3. Iron meshes were placed on both sides of the PHV membrane as electrodes, which possess pore structures to facilitate the direct contact of sound waves with the membrane. During the propagation of the sound wave, different air pressures were generated on both sides of the PHV membrane, leading to its continuous vibrations and bending toward the iron mesh, as well as collisions between the inner PDMS valves and PVDF fibers, resulting in piezo−triboelectric output. The specific charge transfer process is as follows: Initially, in an equilibrium state, the membrane is neither bending nor contacting the mesh, so no charge transfer occurs in the external circuit (Figure 3a). Once the membrane deforms from sound waves, under the piezoelectric effect, different charges accumulate on the upper and lower surfaces of the membrane due to the change in the dipole moment.[30] Furthermore, the deformation of the film causes contact between PDMS valves and PVDF fibers, leading to extra charge transfer because of the triboelectric effect and their different ability to bind electrons.[31] Then, under the effect of electrostatic induction, the lower mesh closer to the membrane gains electrons and becomes negatively charged (Figure 3b). Due to the inherent characteristics of sound waves, the film will gradually recover from the deformation and move away from the electrode. As a result, the electric potential generated by the deformation gradually disappears and the induced charges no longer accumulate on one electrode.[32] The reverse flow of the electrons to balance the potential of the meshes creates a reverse current in the external circuit (Figure 3c). It is worth mentioning that, thanks to the insulating properties of the polymer, the charges generated in the membrane by triboelectrification will be retained during this process.[33,34] Subsequently, the membrane is again deformed by the reverse force of the sound wave and the inner PDMS valve comes into physical contact with PVDF fiber as well, resulting in a similar but reverse charge transfer process (Figure 3d,e). On account of the nanoporous and hollow fiber structure, the PHV membrane has a lower Young's modulus than traditional PVDF fiber film, resulting in stronger vibration and greater deformation under the same acoustic stimulation, which in turn leads to a higher piezo−triboelectric output.[35,36] The PDMS valves also make an enormous contribution. In conjunction with the above factors, the proposed PHVAH exhibits admirable sound collection capabilities. The quantity of charge transferred in one cycle was measured to be 33.8 nC, corresponding to a transferred surface charge density of 48.3 μC m^{-2}.

The load capacity of PHVAH is crucial in realizing practical applications, and thus, the output performance was monitored under different external loads. As the resistance increases from 10 Ω to 100 MΩ, the corresponding output current of PHVAH decreases from 16.6 to 3.6 μA, while the output voltage displays an opposite behavior (Figure 4a). With an external resistance of 10 MΩ, PHVAH generates an instantaneous maximum power of 0.65 mW, corresponding

https://doi.org/10.1021/acsami.1c04489
ACS Appl. Mater. Interfaces 2021, 13, 26981−26988

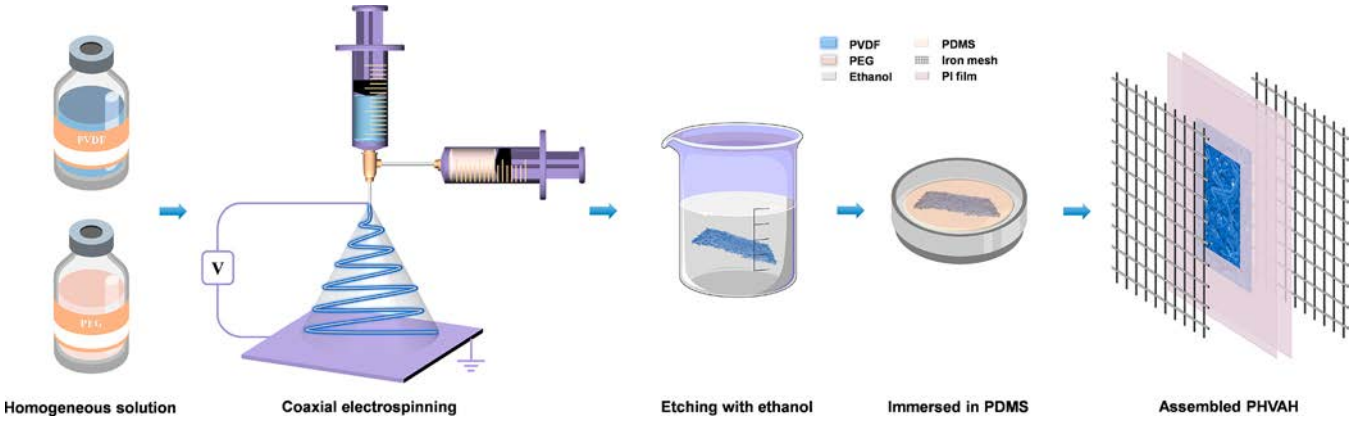

Figure 5. Schematic diagram of the fabrication procedure of PHVAH.

to a maximum areal power density of 0.92 W m^{-2} (Figure 4b). The introduction of PDMS not only improves the sensitivity of the PHVAH as discussed above but also extraordinarily strengthens the durability and cycle reliability (Figure S7) by virtue of its excellent flexibility and stability.

Holding a collection of the above superior performance and simpler structure, the PHVAH proposed here has great potential in the practical application of sound detection and collection (Tables S1−S3). To verify this inference, a practical application can be demonstrated. As shown in Video S1, PHVAH can not only detect the sound but also even output a continuously changing electrical signal output (Figure 4d,e) in real time following the change of the music (Figure 4c). Moreover, the energy collected from the acoustic and converted by the PHVAH is strong enough to light up seven blue bulbs connected into series in a 'V' shape (Figure 4f and Video S2), and Video S3 shows the LED bulbs flickering along with the rhythm of the audio. Ultrahigh sensitivity, broad working frequency band, and satisfying stability and flexibility make PHVAH an ideal solution for detecting, recording, and collecting sound energy and providing a realistic significance for a larger scale of acoustic harvesting and self-powered portable electronics in the future.

3. CONCLUSIONS

In this work, by innovatively employing nanoporous PVDF hollow nanofibers and the PDMS valve structure, PHVAH prepared by coaxial electrospinning has emerged as a new paradigm for fabricating efficient acoustic collectors. Utilizing piezoelectricity and triboelectricity, the PHVAH distinguishes itself in terms of performance in several major aspects. The inherent characteristics of electrospinning and the design of hollow structures endow the PHV membrane with rich porosity, resulting in a large specific surface area and low Young's modulus, thereby generating increased piezo−triboelectric output. Besides, the PDMS valves enlarge the vibration of the membrane under sound waves and generate additional friction with PVDF fibers, further raising the performance of PHVAH. The effects of the concentrations of PVDF, PEG, and PDMS, the decibel and frequency of sound, and the working distance on device performance were extensively investigated. The optimum output of PHVAH was clearly identified as 105.5 V and 16.7 μA when an acoustic stimulus of 117.6 dB and 150 Hz was applied. The converted charge density was 48.3 μC m^{-2}, corresponding to an areal power density of 0.92 W m^{-2}. The PHVAH can detect sound changes in a song in real time and even further convert the sound energy into electrical energy, enough to light up seven series-connected blue LED bulbs. Holding a collection of superior performances, including high sensitivity, broad working frequency range, together with superior stability and flexibility, the PHVAH is distinct and unique in sound recording and acoustic harvesting and could expand the opportunities for extensive self-powered IoT applications with guaranteed performance.

4. EXPERIMENTAL SECTION

Preparation of the Nanoporous PVDF Hollow Fiber Membrane with PDMS Valve. The nanoporous PVDF hollow fiber membrane was successfully fabricated by coaxial spinning. A core−sheath layer was first formed using two immiscible materials, and then, the core was removed by etching to prepare the porous and hollow structured fibers. The specific steps for the fabrication procedure are as follows: (1) Prepare the materials. The PVDF sheath solution (10%−20% w/v) was obtained by dissolving PVDF in a mixed solvent of *N*,*N*-dimethylacetamide (DMF) and acetone (at a ratio of 1:1). Then, PEG was dissolved in tetrahydrofuran (THF) through ultrasound to prepare the core solution (20%−30% w/v), which was used as sacrificial layer. Then, the prepared sheath and core solution were fed into 10 mL standard syringes, which were connected to the corresponding needles by Teflon tubes. (2) Coaxial electrospinning of the PVDF/PEG core−sheath fiber membrane. The PVDF and PEG solutions were delivered at 8 and 2 μL min^{-1} via a syringe pump (KD-100). A voltage of ∼13 kV was applied using a high-voltage power supply during the electrospinning process. The positive electrode was subjected directly to the needle, and the negative electrode was clamped to the platform wrapped in tin foil for the collection of nanofibers. The gap between needle tip and the platform was 15 cm. The spinning was performed at a room temperature of 25 °C, and the electrospun PVDF/PEG core−sheath membrane was dried in a vacuum at 80 °C for 8 h to fully remove the solvent DMF. (3) Etch to obtain a nanoporous PVDF hollow fiber membrane. The core material PEG was removed by soaking the PVDF/PEG core−sheath membrane in absolute ethanol for 12 h. (4) Form PDMS valves inside the membrane. PDMS solution was obtained by uniformly mixing a PDMS and a curing agent at a ratio of 10:1 and then diluting the mixture in toluene (0.1%−0.5% w/v). The nanoporous PVDF hollow fiber membrane was immersed in the PDMS solution and evacuated to form PDMS valves in the gaps and holes of the nanoporous PVDF hollow fiber. Then, the PDMS was cured at 80 °C for 2 h. On the basis of the steps above, a nanoporous PVDF hollow fiber membrane with PDMS valves was prepared.

Assembly of the PHVAH. The PHV membrane was cut into 4.5 cm × 3 cm rectangles and fixed between two polyimide films (10 cm × 10 cm, with a hole of 3.5 cm × 2 cm). The polyimide films were set to separate the outermost iron meshes (10 cm × 10 cm; wire diameter, 0.2 mm; density, 400 mesh), which serve as the positive and

https://doi.org/10.1021/acsami.1c04489
ACS Appl. Mater. Interfaces 2021, 13, 26981−26988

negative electrodes, to avoid short circuits. The fabrication procedure and structure of the PHVAH are illustrated in Figure 5 and Figure S8.

Measurement of the PHVAH. A signal sampling PXI system (Quad-core embed controller, NI PXIe-8135; Chassis, NI PXIe-1082; Acquisition card, NI PXIe-4499, National Instruments) and an electrometer (Keithley 6517B) were taken to test the electrical output under the stimulation of sound, which serves as an index to evaluate the acoustic collection capability of the PHVAH.

Characterization. The fiber morphologies of the samples were investigated via a field emission scanning electron microscope (JSM-7600F, JEOL Co., Ltd.). A thickness gauge (033004, EXPLOIT Co., Ltd.) was employed to measure the thickness of the membranes. Besides, an X-ray diffractometer (X'Pert3 powder, PANalytical B.V.) and a Fourier transform infrared spectrometer (VERTEX 70 Bruker) were used to carry out phase analysis.

■ ASSOCIATED CONTENT

Supporting Information

The Supporting Information is available free of charge at https://pubs.acs.org/doi/10.1021/acsami.1c04489.

Figures of SEM images, surface morphology, FTIR spectra, output current, SPL polar plots, output voltage, and structure illustration and physical photos of PHVAH device, calculation of sound pressure, and tables of summary of the PENG and TENG perfomance in the literature and sound pressure level of various sound sources (PDF)

Video of electrical signal response of PHVAH when playing a piece of music (MP4)

Video of seven blue LED bulbs connected into a series in a 'V' shape illuminated directly by the PHVAH (MP4)

Video of LED bulbs powered by the PHVAH flickers along with the rhythm of the audio (MP4)

■ AUTHOR INFORMATION

Corresponding Author

Yunming Wang − *State Key Laboratory of Materials Processing and Die & Mould Technology, School of Materials Science and Engineering, Huazhong University of Science and Technology, Wuhan 430074, China;* orcid.org/0000-0002-8557-0349; Phone: +86 027 87543492; Email: wang653@hust.edu.cn

Authors

Zhaohan Yu − *State Key Laboratory of Materials Processing and Die & Mould Technology, School of Materials Science and Engineering, Huazhong University of Science and Technology, Wuhan 430074, China*

Ming Chen − *State Key Laboratory of Materials Processing and Die & Mould Technology, School of Materials Science and Engineering, Huazhong University of Science and Technology, Wuhan 430074, China*

Jiaqi Zheng − *State Key Laboratory of Materials Processing and Die & Mould Technology, School of Materials Science and Engineering, Huazhong University of Science and Technology, Wuhan 430074, China*

Yongkang Zhang − *School of Mechanical and Electronic Engineering, Jingdezhen Ceramic Institute, Jingdezhen 333403, P. R. China*

Huamin Zhou − *State Key Laboratory of Materials Processing and Die & Mould Technology, School of Materials Science and Engineering, Huazhong University of Science and Technology, Wuhan 430074, China*

Dequn Li − *State Key Laboratory of Materials Processing and Die & Mould Technology, School of Materials Science and Engineering, Huazhong University of Science and Technology, Wuhan 430074, China*

Complete contact information is available at: https://pubs.acs.org/10.1021/acsami.1c04489

Notes

The authors declare no competing financial interest.

■ ACKNOWLEDGMENTS

H.Z. acknowledges the financial support from the National Key Research and Development Program of China (Grant No. 2018YFB1106700). Z.Y., Y.W., and J.Z. acknowledge the General Program of National Natural Science Foundation of China (52075196) for the financial support. Y.W. would like to thank the Double First-Class-Independent Innovation-Subject Construction (5001110032) for support. H.Z. and Y.W. gratefully acknowledge financial support provided by the Fundamental Research Funds for the Central Universities (Grant No. 2016YXZD059).

■ ABBREVIATIONS

PVDF, polyvinylidene fluoride
PDMS, polydimethylsiloxane
AH, acoustic harvester
PH, PVDF hollow fiber
PHV, PVDF hollow fiber and PDMS valve
PVDFAH, PVDF fiber based acoustic harvester
PHAH, PVDF hollow fiber based acoustic harvester
PHVAH, PVDF hollow fiber and PDMS valve based acoustic harvester

■ REFERENCES

(1) Shi, B.; Li, Z.; Fan, Y. Implantable Energy-Harvesting Devices. *Adv. Mater.* **2018**, *30* (44), 1801511.

(2) Ahmed, A.; Hassan, I.; El-Kady, M. F.; Radhi, A.; Jeong, C. K.; Selvaganapathy, P. R.; Zu, J.; Ren, S.; Wang, Q.; Kaner, R. B. Integrated Triboelectric Nanogenerators in the Era of the Internet of Things. *Advanced Science* **2019**, *6* (24), 1802230.

(3) Li, W.; Torres, D.; Díaz, R.; Wang, Z.; Wu, C.; Wang, C.; Lin Wang, Z.; Sepúlveda, N. Nanogenerator-based Dual-functional and Self-powered Thin Patch Loudspeaker or Microphone for Flexible electronics. *Nat. Commun.* **2017**, *8* (1), 15310.

(4) Cheng, L.; Xu, Q.; Zheng, Y.; Jia, X.; Qin, Y. A Self-improving Triboelectric Nanogenerator with Improved Charge Density and Increased Charge Accumulation Speed. *Nat. Commun.* **2018**, *9* (1), 3773.

(5) Jung, Y. H.; Park, B.; Kim, J. U.; Kim, T.-i. Bioinspired Electronics for Artificial Sensory Systems. *Adv. Mater.* **2019**, *31* (34), 1803637.

(6) Sun, P.; Jiang, S.; Huang, Y. Nanogenerator as Self-powered Sensing Microsystems for Safety Monitoring. *Nano Energy* **2021**, *81*, 105646.

(7) Sun, B.; Li, X.; Zhao, R.; Ji, H.; Qiu, J.; Zhang, N.; He, D.; Wang, C. Electrospun Poly(vinylidene fluoride)-zinc Oxide Hierarchical Composite Fiber Membrane as Piezoelectric Acoustoelectric Nanogenerator. *J. Mater. Sci.* **2019**, *54*, 2754−2762.

(8) Yuan, M.; Cao, Z.; Luo, J.; Chou, X. Recent Developments of Acoustic Energy Harvesting: A Review. *Micromachines* **2019**, *10* (1), 48.

(9) Sultana, A.; Alam, M. M.; Ghosh, S. K.; Middya, T. R.; Mandal, D. Energy Harvesting and Self-powered Microphone Application on Multifunctional Inorganic-organic Hybrid Nanogenerator. *Energy* **2019**, *166*, 963−971.

(10) Cui, N.; Jia, X.; Lin, A.; Liu, J.; Bai, S.; Zhang, L.; Qin, Y.; Yang, R.; Zhou, F.; Li, Y. Piezoelectric Nanofiber/polymer Composite Membrane for Noise Harvesting and Active Acoustic Wave Detection. *Nanoscale Advances* **2019**, *1* (12), 4909−4914.
(11) Pang, Y.; Chen, S.; An, J.; Wang, K.; Deng, Y.; Benard, A.; Lajnef, N.; Cao, C. Multilayered Cylindrical Triboelectric Nanogenerator to Harvest Kinetic Energy of Tree Branches for Monitoring Environment Condition and Forest Fire. *Adv. Funct. Mater.* **2020**, *30* (32), 2003598.
(12) Hao, C.; He, J.; Zhai, C.; Jia, W.; Song, L.; Cho, J.; Chou, X.; Xue, C. Two-dimensional Triboelectric-electromagnetic Hybrid Nanogenerator for Wave Energy Harvesting. *Nano Energy* **2019**, *58*, 147−157.
(13) Yu, Z.; Wang, Y.; Zheng, J.; Xiang, Y.; Zhao, P.; Cui, J.; Zhou, H.; Li, D. Rapidly Fabricated Triboelectric Nanogenerator Employing Insoluble and Infusible Biomass Materials by Fused Deposition Modeling. *Nano Energy* **2020**, *68*, 104382.
(14) Yu, S.; Zhang, Y.; Yu, Z.; Zheng, J.; Wang, Y.; Zhou, H. PANI/PVDF-TrFE Porous Aerogel Bulk Piezoelectric and Triboelectric Hybrid Nanogenerator Based on In-situ Doping and Liquid Nitrogen Quenching. *Nano Energy* **2021**, *80*, 105519.
(15) Zheng, J.; Wang, Y.; Yu, Z.; Fu, Y.; Chen, D.; Zhao, P.; Zhou, H. Integrated Nanospheres Occupancy-removal and Thermoforming into Bulk Piezoelectric and Triboelectric Hybrid Nanogenerators with Inverse Opal Nanostructure. *Nano Energy* **2019**, *64*, 103957.
(16) Shepelin, N. A.; Glushenkov, A. M.; Lussini, V. C.; Fox, P. J.; Dicinoski, G. W.; Shapter, J. G.; Ellis, A. V. New Developments in Composites, Copolymer Technologies and Processing Techniques for Flexible Fluoropolymer Piezoelectric Generators for Efficient Energy Harvesting. *Energy Environ. Sci.* **2019**, *12* (4), 1143−1176.
(17) Chen, F.; Wu, Y.; Ding, Z.; Xia, X.; Li, S.; Zheng, H.; Diao, C.; Yue, G.; Zi, Y. A Novel Triboelectric Nanogenerator based on Electrospun Polyvinylidene Fluoride Nanofibers for Effective Acoustic Energy Harvesting and Self-powered Multifunctional Sensing. *Nano Energy* **2019**, *56*, 241−251.
(18) Sultana, A.; Mehebub Alam, M.; Sadhukhan, P.; Ghorai, U. K.; Das, S.; Middya, T. R.; Mandal, D. Organo-lead Halide Perovskite Regulated Green Light Emitting Poly(vinylidene fluoride) Electrospun Nanofiber Mat and its Potential Utility for Ambient Mechanical Energy Harvesting Application. *Nano Energy* **2018**, *49*, 380−392.
(19) Lang, C.; Fang, J.; Shao, H.; Wang, H.; Yan, G.; Ding, X.; Lin, T. High-output Acoustoelectric Power Generators from Poly(vinylidenefluoride-co-trifluoroethylene) Electrospun Nano-nonwovens. *Nano Energy* **2017**, *35*, 146−153.
(20) Zhang, L.; Liao, Y.; Wang, Y.-C.; Zhang, S.; Yang, W.; Pan, X.; Wang, Z. L. Cellulose II Aerogel-Based Triboelectric Nanogenerator. *Adv. Funct. Mater.* **2020**, *30*, 2001763.
(21) Ahmad, I.; Hassan, A.; Anjum, M. U.; Malik, S.; Ali, T. Ambient Acoustic Energy Harvesting using Two Connected Resonators with Piezoelement for Wireless Distributed Sensor Network. *Acoust. Phys.* **2019**, *65* (5), 471−477.
(22) Zhao, H.; Xiao, X.; Xu, P.; Zhao, T.; Song, L.; Pan, X.; Mi, J.; Xu, M.; Wang, Z. Dual-Tube Helmholtz Resonator-Based Triboelectric Nanogenerator for Highly Efficient Harvesting of Acoustic Energy. *Adv. Energy Mater.* **2019**, *9*, 1902824.
(23) Zeng, Q.; Wu, Y.; Tang, Q.; Liu, W.; Wang, X.; et al. A High-efficient Breeze Energy Harvester Utilizing a Full-packaged Triboelectric Nanogenerator Based on Flow-induced Vibration. *Nano Energy* **2020**, *70*, 104524.
(24) Parida, K.; Thangavel, G.; Cai, G.; Zhou, X.; Park, S.; Xiong, J.; Lee, P. S. Extremely Stretchable and Self-healing Conductor Based on Thermoplastic Elastomer for All-three-dimensional Printed Triboelectric Nanogenerator. *Nat. Commun.* **2019**, *10* (1), 2158.
(25) Shawon, S. M. A. Z.; Sun, A. X.; Vega, V. S.; Chowdhury, B. D.; Uddin, M. J.; et al. Piezo-Tribo Dual Effect Hybrid Nanogenerators for Health Monitoring. *Nano Energy* **2021**, *82*, 105691.
(26) Abdolmaleki, H.; Agarwala, S. PVDF-BaTiO 3 Nanocomposite Inkjet Inks with Enhanced β-Phase Crystallinity for Printed Electronics. *Polymers* **2020**, *12* (10), 2430.
(27) Cai, X.; Lei, T.; Sun, D.; Lin, L. A Critical Analysis of the α, β and γ Phases in Poly(vinylidene fluoride) using FTIR. *RSC Adv.* **2017**, *7* (25), 15382−15389.
(28) Xu, L.; Pang, Y.; Zhang, C.; Jiang, T.; Chen, X.; Luo, J.; Tang, W.; Cao, X.; Wang, Z. L. Integrated triboelectric nanogenerator array based on air-driven membrane structures for water wave energy harvesting. *Nano Energy* **2017**, *31*, 351−358.
(29) Gong, S.; Zhang, B.; Zhang, J.; Wang, Z. L.; Ren, K. Biocompatible Poly(lactic acid)-Based Hybrid Piezoelectric and Electret Nanogenerator for Electronic Skin Applications. *Adv. Funct. Mater.* **2020**, *30* (14), 1908724.
(30) Yuan, X.; Gao, X.; Shen, X.; Yang, J.; Li, Z.; Dong, S. A 3D-printed, alternatively tilt-polarized PVDF-TrFE polymer with enhanced piezoelectric effect for self-powered sensor application. *Nano Energy* **2021**, *85*, 105985.
(31) Zhu, G.; Pan, C.; Guo, W.; Chen, C.-Y.; Zhou, Y.; Yu, R.; Wang, Z. L. Triboelectric-Generator-Driven Pulse Electrodeposition for Micropatterning. *Nano Lett.* **2012**, *12* (9), 4960−4965.
(32) Wang, Z. L.; Jiang, T.; Xu, L. Toward the blue energy dream by triboelectric nanogenerator networks. *Nano Energy* **2017**, *39*, 9−23.
(33) Zhu, G.; Lin, Z.-H.; Jing, Q.; Bai, P.; Pan, C.; Yang, Y.; Zhou, Y.; Wang, Z. L. Toward Large-Scale Energy Harvesting by a Nanoparticle-Enhanced Triboelectric Nanogenerator. *Nano Lett.* **2013**, *13* (2), 847−853.
(34) Wang, Z. L. Triboelectric Nanogenerators as New Energy Technology for Self-Powered Systems and as Active Mechanical and Chemical Sensors. *ACS Nano* **2013**, *7* (11), 9533−9557.
(35) Sahu, M.; Vivekananthan, V.; Hajra, S.; Khatua, D. K.; Kim, S.-J. Porosity Modulated Piezo-triboelectric Hybridized Nanogenerator for Sensing Small Energy Impacts. *Applied Materials Today* **2021**, *22*, 100900.
(36) Zheng, Q.; Fang, L.; Guo, H.; Yang, K.; Cai, Z.; Meador, M. A. B.; Gong, S. Highly Porous Polymer Aerogel Film-Based Triboelectric Nanogenerators. *Adv. Funct. Mater.* **2018**, *28* (13), 1706365.

https://doi.org/10.1021/acsami.1c04489
ACS Appl. Mater. Interfaces 2021, 13, 26981−26988